PENSOFT
SENCKENBERG world of biodiversity
Leibniz Association

New species of the long-horned caddisfly *Oecetis* McLachlan, 1877 (Trichoptera: Leptoceridae) from the Atlantic Forest, Brazil and their evolutionary relationship

Pedro Bonfá-Neto[1,2], Frederico Falcão Salles[1], Albane Vilarino[3]

1 *Museu de Entomologia, Departamento de Entomologia, Universidade Federal de Viçosa, Av. P.H. Rolfs, s.n, Campus Universitário, CEP 36570-900, Viçosa, MG, Brazil*

2 *Programa de Pós-graduação em Entomologia, Universidade Federal de Viçosa, Av. P.H. Rolfs, s.n, Campus Universitário, CEP 36570-900, Viçosa, MG, Brazil*

3 *Universidade Federal da Bahia, Instituto de Biologia, Rua Barão de Geremoabo, 147, Ondina, CEP 40170–115, Salvador, BA, Brazil*

https://zoobank.org/26E03DFA-E670-4562-A652-26F1C180B3B2

Corresponding author: Pedro Bonfá Neto (bonfa.pn@gmail.com)

Received 17 October 2023
Accepted 17 June 2024
Published 2 july 2024

Academic Editors Steffen Pauls, Marianna Simões

Citation: Bonfá-Neto P, Salles FF, Vilarino A (2024) New species of the long-horned caddisfly *Oecetis* McLachlan, 1877 (Trichoptera: Leptoceridae) from the Atlantic Forest, Brazil and their evolutionary relationship. Arthropod Systematics & Phylogeny 82: 551–566. https://doi.org/10.3897/asp.82.e114286

Abstract

Asymmetrical genitalia are reported from major Trichoptera subgroups and evolved multiple times independently. In *Oecetis*, it is a characteristic of the *insconpicua* group. However, certain species in other species groups also evolved an asymmetrical spiny projection on the phallotheca. Here, two new species with an asymmetric projection are described in the *falicia* group from the Brazilian Atlantic Forest, Espírito Santo state. Their phylogenetic relationships were investigated through a Bayesian analysis combining COI and morphological data. Additionally, we provide new records of *Oecetis connata*, *O. inconspicua* and *O. paranensis* from the Espírito Santo state, and *O. connata* and *O. flinti* from Minas Gerais state. ***Oecetis capixaba* sp. nov.** is placed with low support as the sister species of *O. acanthostema*, both presenting stout spine-like setae on the inner surface of the inferior appendage; the new species is diagnosed by the long spine-like setae on the inferior appendage, the narrow dorsolateral process of segment IX, and the phallic apparatus without apical projections. ***Oecetis ruschii* sp. nov.** is placed as a sister group of the clade including *O. facilia* and *O. furcata*, both presenting forked dorsolateral processes of segment IX; the new species is diagnosed by the dorsolateral process of segment IX with a lateral branching and the apex of inferior appendage wide and triangular. While the phylogenetic results should be considered preliminary and interpreted with caution, they indicate that the asymmetric projection evolved multiple times convergently in the *avara*, *punctata*, and *falicia* groups. The asymmetric genitalia in the *falicia* group seems to have evolved only in males since no correspondent asymmetry is described for females. The function of the asymmetrical projection remains unknown.

Key words

Aquatic insects, Asymmetric genitalia, Bayesian inference, Diversity, Neotropical

1. Introduction

Oecetis McLachlan, 1877 is the only member of the tribe Oecetini Silfvenius, 1905 of the family Leptoceridae Leach, 1815. The genus is distributed worldwide, with their immatures inhabiting major rivers and lotic environments where they usually are very common and abundant (Schmid 1998). Their larvae have strong mandibles and

a strict predaceous habit (Wallace et al. 2003; Wiggins 2007). Currently, there are around 600 species of *Oecetis* (Johanson et al. 2020a, 2020b; Morse 2023), 73 of which occur in the Neotropical region (Quinteiro and Almeida 2021).

The relationship among the long-horned caddisflies (Leptoceridae) was investigated by Malm and Johanson (2011) through molecular data. In their preferred hypothesis, *Oecetis* was placed as the sister group of Triaenodini + Mystacidini + Setodini. The time-calibrated tree of Thomas et al. (2020) suggests Leptoceridae originated in the early Cretaceous (120 Mya), the radiation of taxa more closely related to *Oecetis* is inferred to the Paleocene (around 60 Mya). However, a fossil case from the early Cretaceous of Australia (122.46 to 112.6 Mya) is a possible *Oecetis* specimen (Jell and Duncan 1986).

Several species groups have been proposed for *Oecetis* (Neboiss 1989; Chen 1993; Schmid 1998; Wells 2000, 2004, 2006; Malicky 2005). Neotropical species were traditionally placed in six of them: *avara*, *punctata*, *inconspicua*, *punctipennis*, *testacea*, and *falicia* groups (Blahnik and Holzenthal 2014; Quinteiro and Holzenthal 2017). The *avara* group occurs from the Nearctic to northern South America and is identified by the mitten-shaped inferior appendages (Blahnik and Holzenthal 2014); the *punctata* group is strictly Neotropical and diagnosed by the quadrate inferior appendage with apical processes; the *inconspicua* group occurs in all regions and is diagnosed by the round phallic apparatus bearing a ventral projection and helical phallic spine; the *punctipennis* group has an austral distribution (South America, Australia) and can be diagnosed by the forewing R1+2 vein splitting very close to the wing margin; the *testacea* group occur in all regions and is characterized by the honeycomb microstructure on the abdominal terga V–VIII; the *falicia* group (also referred as *Quaria* group (Milne 1934; Chen 1993; Quinteiro and Calor 2015)) is widespread and characterized by the presence of dorsolateral processes on segment IX and reduced tergum IX (Chen 1993; Quinteiro and Holzenthal 2017).

The phylogenetic relationship of the Neotropical *Oecetis* was investigated through morphological characters by Quinteiro and Almeida (2021). The characters distinguishing *Oecetis* from other Leptocerinae were the unbranched forewing M vein and the short phallic apparatus (although the latter is reverted in some lineages). Their phylogenetic hypothesis indicated that the Neotropical species do not form a monophyletic group, but rather had an intricate evolutionary history with lineages originating in other biogeographic regions. This suggests an ancient radiation of *Oecetis*, possibly before the continents fully separated (Quinteiro and Almeida 2021), contrary to the Paleocene age previously estimated (Malm et al. 2013; Thomas et al. 2020). The *Oecetis* phylogeny recovered most of the taxonomically defined species groups (Quinteiro and Almeida 2021). However, the *avara* group was paraphyletic in relation to the *punctata* group, and the *testacea* group was polyphyletic. Additionally, Quinteiro and Almeida (2021) proposed the *pratti* group, occurring in the Antilles and South America. They are characterized by the forewing s and r–m crossveins aligned and the cylindrical dorsal lobe of tergum X with clavate apex (Quinteiro and Almeida 2021).

Here we describe and illustrate two additional *falicia* group species from the Atlantic Forest, Brazil. Both new species present a conspicuous asymmetrical process on the phallic apparatus. Asymmetrical genitalia have been observed in all major Trichoptera lineages and have evolved convergently numerous times (Huber et al. 2007). In *Oecetis*, an asymmetrical phallic apparatus is a diagnostic character of the *O. inconspicua* group (Quinteiro and Almeida 2021). In order to investigate the evolutionary relationship between the new species and the evolution of the asymmetrical processes, we included the new species and other similar species from the *falicia* group in a cladistic analysis combining the morphologic dataset of Quinteiro and Almeida (2021), and available DNA barcodes (mitochondrial cytochrome C oxidase subunit 1).

2. Material and methods

2.1. Collection, specimen preparation, illustrations, and depositories

The specimens were collected with various types of light traps (UV pan traps, Pennsylvania traps, and light over a white cloth) or Malaise traps as indicated in the material analyzed sections. The morphological terminology follows Quinteiro and Holzenthal (2017). Paired structures were referred to in the singular form in the descriptions. The genitalia were studied after removing the abdomens of the examined specimens and clearing them using 85% lactic acid, as outlined by Blahnik et al. (2007). The prepared genitalia samples were transferred to microvials with 80% ethanol, and later were placed in depression slides with a drop of glycerin and examined using a compound microscope (Olympus CX31) at 100–400X magnification. Photographs were taken using a Motic Camera (Moticam A5) attached to the microscope. The photographs were stacked using the Helicon Focus® software and used as templates for the illustrations, which were made by tracing the structures digitally using Adobe Illustrator® CS6. Material examined, including types of the new species, are deposited in the Museu de Entomologia, Universidade Federal de Viçosa (UFVB), supplementary material (File S1).

2.2. Phylogenetic analyses

For the phylogenetic placement of the new species we modified the morphological matrix of Quinteiro and Almeida (2021). We included 10 additional species to the original matrix (*Oecetis capixaba* **sp. nov.**; *O. ruschii* **sp. nov.**; *O. catagua* Henriques-Oliveira et al., 2018; *O. furcata* Quinteiro & Calor, 2015; *O. acanthostema* Quinteiro

Table 1. List of morphological characters and states, for *Oecetis* and related taxa. (Modified from Quinteiro and Almeida (2021), character numbers as in the original publication).

	Character list and states:
0	Forewing, M vein: (0) Branched into M 1+2 and M 3+4 ; (1) Unbranched.
1	Middle leg femur, row of spines on the inner surface: (0) Absent; (1) Present.
2	Middle leg femur spines, coverage area: (0) The whole podomere; (1) Half of the podomere length.
3	Hind leg tibia, row of spines on the inner surface: (0) Absent; (1) Present.
4	Hind leg tibia spines, coverage area: (0) The whole podomere; (1) Half of the podomere length.
5	Foreleg tibia, apical spur: (0) Absent; (1) Present.
6	Forewing, fork V: (0) Rooted; (1) Sessile; (2) Petiolate.
7	Forewing,sectoral crossvein (r 2+3 –r 4+5) alignment to the r–m crossvein: (0) Aligned; (1) not-aligned.
8	Hind wing, Rs sector on the hind wing: (0) Absent; (1) Present.
9	Hind wing, fork I: (0) Absent; (1) Present.
10	Forewing, setae fringe on the inner surface: (0) Absent; (1) Present.
11	Forewing, end of Sc vein: (0) Vestigial; (1) Whole.
12	Forewing, black spots at the end of veins, forks and junctions on the membrane: (0) Absent; (1)Present.
13	Forewing, dark bands on the membrane around the cord: (0) Absent; (1) Present.
14	Forewing, apex: (0) Rounded; (1) Acuminated.
15	Hind wing, position of r–m crossvein related to the fork between M 1+2 and M 3+4: (0) Rooted; (1) Sessile; (2) Petiolate.
16	Forewing, fork I in relation to the discoidal cell crossvein: (0) Rooted; (1) Sessile; (2) Petiolate.
17	Forewing, depth of the fork I: (0) Shallow; (1) Deep.
18	Hind wing, anal region: (0) Wide (as in *Ceraclea* and *Athripsodes*); (1) Narrow (as in *Brachysetodes* and *Setodes*).
19	Tergum IX related to the sternum IX, length: (0) Longer than sternum IX; (1) same length of sternum IX; (2) shorter than sternum IX.
20	Terga V to VIII honeycomb texture: (0) Absent; (1) Present.
21	Tergum IX and X, acrotergite: (0) Absent; (1) Present.
22	Tergum IX and X acrotergite, number: (0) One; (1) Two.
23	Segment IX, dorsolateral processes: (0) Absent; (1) Present.
24	Segment IX, dorsolateral processes curvature: (0) Straight; (1) Bent ventrally.
25	Segment IX, dorsolateral processes relative length: (0) As long as the preanal appendages; (1) Much longer than the preanal appendages.
26	Segment IX, dorsolateral processes shape: (0) Thread-like; (1) Forked.
27	Preanal appendage fusion: (0) Completely fused to each other; (1) Not fused to each other; (2) Partially fused to each other.
28	Preanal appendages, shape in dorsal view: (0) Ovoid; (1) Digitate.
29	Tergum X, dorsal lobe: (0) Absent; (1) Present.
30	Tergum X, dorsal lobe shape: (0) Cylindrical throughout length; (1) Cylindrical with globose apex; (2) Flat; (3) Saddle-shaped.
31	Tergum X, median incision: (0) Absent (undivided tergum X); (1) Present (divided tergum X).
32	Tergum X, lobes of divided tergum, shape in dorsal view: (0) Rod-like; (1) Broad at base and tapering distally.
33	Tergum X, apex: (0) Truncate; (1) Acuminate; (2) Irregular shape; (3) Round.
34	Tergum X median incision shape: (0) V-shaped shallow; (1) V-shaped deep; (2) U-shaped.
35	Inferior appendages, length: (0) Short; (1) Long.
36	Inferior appendages, dorsal lobe: (0) Absent; (1) Present.
37	Inferior appendages, dorsal lobe shape: (0) Quadrate; (1) Ovoid; (2) Digitate; (3) Triangular; (4) L-shaped.
38	Inferior appendages, dorsal lobe insertion: (0) Inner margin; (1) Laterally.
39	Inferior appendages, dorsal lobe orientation angle: (0) Projecting upward (90 degrees to the distal portion); (1) Projecting distally (less than 90 degrees to the distal portion).
40	Inferior appendages, ventral lobe: (0) Absent; (1) Present.
41	Inferior appendages, ventral lobe shape: (0) Quadrate; (1) Digitate; (2) Triangular; (3) acute
42	Inferior appendages, ventral lobe size: (0) Small (less than 1/4 length of distal portion); (1) big (more than 1/4 length of distal lobe).
43	Inferior appendages, general shape: (0) Cylindrical with apex rounded; (1) Tapering distally with apex acute; (2) Short and “fist-like”; (3) Cylindrical proximally, enlarged distally.
44	Inferior appendages, when short, fist-like, distal lobe shape: (0) ovoid, ear-like with smooth and rounded edges; (1) quadrate with thick setae on apex; (2) Cylindrical and stout.
45	Inferior appendages, distal lobe, apical incision: (0) Absent; (1) Present.
46	Inferior appendages, distal lobe apical incision, shape in lateral view: (0) V-shaped; (1) L-shaped.
47	Inferior appendages, inner lobe: (0) Absent; (1) Present.
48	Segment IX, posterolateral margin, setae: (0) Absent; (1) Present.
49	Inferior appendages, thick spine-like setae: (0) Absent; (1) Present.
50	Phallic apparatus, symmetry in dorsal view: (0) Symmetrical; (1) Asymmetrical.
51	Phallic apparatus, length: (0) Short; (1) Elongated.
52	Phallic apparatus, when short, shape: (0) Comma-shaped, strongly bent ventrally; (1) Round, inflated; (2) Cylindrical, slightly bent ventrally.

	Character list and states:
53	Phallic apparatus, when short, ventrodistal lamellate process: (0) Absent; (1) Present.
54	Phallic apparatus, endotheca, size: (0) Small (less than 1/3 the phallus volume); (1) Large (more than 1/3 the phallus volume).
55	Phallic apparatus, endotheca, number of lobules: (0) One; (1) Two.
56	Phallic apparatus, additional sclerotized structure in phallic apparatus (other than phallic spine or phallotremal sclerite): (0) Absent; (1) Present.
57	Phallic apparatus, phallic spines: (0) Absent; (1) Present.
58	Phallic apparatus, phallic spines, number: (0) One; (1) Two; (2) Three.
59	Phallic apparatus, phallic spines, shape: (0) Straight; (1) Curved.
60	Phallic apparatus, phallotremal sclerite: (0) Absent; (1) Present.
61	Phallic apparatus, phallotremal sclerite, number: (0) One; (1) Two.
62	Phallic apparatus, phallotheca, asymmetric spine projection: (0) Absent; (1) Present.
63	Phallic apparatus, when short, shape: (0) Comma-shaped, strongly bent ventrally; (1) Round, inflated; (2) Cylindrical, slightly bent ventrally.

& Calor, 2015; *O. acarati* Angrisano & Sganga, 2009; *O. calori* Quinteiro & Holzenthal, 2017; *O. hastapulla* Quinteiro & Holzenthal 2017; *O. machaera* Quinteiro & Holzenthal, 2017; and *O. avara* Banks, 1895), and an additional character corresponding to the asymmetric spine on the phallic apparatus. The final phylogenetic dataset comprised 67 taxa (59 ingroup taxa, 8 outgroup) with 63 morphological characters (Table 1) and sequences of cytochrome oxidase I (COI, 658 bp) available for 30 terminals (Table 2). The original morphological characters and character states (Quinteiro and Almeida 2021) were modified following Sereno's (2007) recommendations. Inapplicable characters were coded as '–'; when the character state was not clear or could not be assessed, it was coded as '?'. Polymorphic characters were treated in the analysis as '?'. Multistate characters were treated as unordered. The original dataset matrix was edited using the software Mesquite 3.8 (Maddison and Maddison 2023).

The phylogeny was based on a probabilistic framework through Bayesian inference as implemented in MrBayes 3.2.7 (Ronquist et al. 2012). The morphological dataset was analyzed using the Mk model (Lewis 2001). To adjust the heterogeneity in rates of evolution across morphological characters, we adopted a homoplasy-based partitioning strategy described by Rosa et al. (2019), which was shown to outperform other approaches for modeling among character rate variation. In this approach the levels of character compatibility are estimated from the relative homoplasy calculated from the consistency index generated in an implied weights parsimony analysis. The parsimony analysis was performed in TNT version 1.6 (Goloboff and Morales 2023). Heuristics searches were performed through 'Traditional Search', with 10,000 replications, three trees saved per replication. In order to segregate the characters according to homoplasy intervals, the adjusted K function implemented in TNT 1.6 was applied, so that the weight ratio between the characters with no homoplasy and the ones with most homoplasy was equal to 10, resulting in a K = 15. Consensus tree of the morphological parsimony analysis is available as supplementary material (File S3). The adjusted values of homoplasy of each character generated in TNT 'character scores' were combined into more inclusive intervals resulting in seven partitions (Table 3). These morphological character partitions were then used in the Bayesian analyses following the parameters indicated in Rosa et al. (2019) (LSET rates = equal; PRSET ratepr = variable, brlenspr = unconstrained:exp(10); LINK shape).

Table 2. Sequences of COI barcode used in the phylogenetic inference, and respective BOLD accession number.

Species	**BOLD accession number**
Athripsodes bergensis	SATRI002-13
Brachysetodes major	UMNEB140-08
Leptocerus americanus	AVMTT037-09
Mystacides interjectus	ABCAD059-08
Nectopsyche argentata	UMNEB177-08
Nectopsyche punctata	GBMIN35590-13
Setodes incertus	BKCAD041-08
Oecetis akimi	GBMNB60844-20
Oecetis amazonica	GBMNB60805-20
Oecetis arizonica	OFCAD375-08
Oecetis avara	HIEPT040-09
Oecetis connata	GBMNB60798-20
Oecetis excisa	GBMNB60809-20
Oecetis iguazu	KKUMN207-10
Oecetis inconspicua	GBMNB60806-20
Oecetis inscripta	UMNEA325-08
Oecetis knutsoni	UMNEB251-08
Oecetis lacustris	BARCO038-14
Oecetis marquesi	TRHGO332-10
Oecetis metlacensis	UMNEA311-08
Oecetis nigropunctata	RUSST215-12
Oecetis ochracea	UMNEB664-08
Oecetis paranensis	KKUMN211-10
Oecetis pechana	AUCAD016-09
Oecetis pratti	OFTRI403-10
Oecetis prolongata	KKUMN212-10
Oecetis pseudoinconspicua	UMNEA332-08
Oecetis punctata	UMNEA333-08
Oecetis punctipennis	GBMNB60810-20
Oecetis testacea	CAUTR083-09

The COI sequences available in the BOLD website (Barcode of life Database) were included to provide additional evidence about taxa relationship. We included in the phylogenetic analyses COI sequence fragments for 30

Table 3. Morphological partitions used for the Bayesian inferences. The partitions were established based on its levels of homoplasy obtained from the adjusted homoplasy of a cladistic analysis under implied weight. Individual values were combined into more inclusive classes.

Partition	Adjusted homoplasy	Characters
1	0	0, 8, 23, 25, 26, 38, 44, 46, 47, 52
2	0.1	9, 24, 27, 42, 55, 19, 20, 22, 58
3	0.2	3, 17, 56, 59, 15, 37, 39, 41, 45, 49, 62, 2, 40, 50, 51
4	0.3	35, 53, 12, 28, 32, 48, 54, 57, 21, 29, 30, 36
5	0.4	7, 34, 6, 31, 43, 5
6	0.5	14, 60, 1, 16, 13, 33
7	—	4, 10, 11, 18, 61

species (Table 2). Given the unavailability of COI data for the outgroup species *Setodes obscurus*, we opted to include this fragment from *S. incertus*. The sequences were aligned using MAFFT through the method L-INS-I (Katoh and Standley 2013), partitioned by codon position, and concatenated with the morphological dataset using SequenceMatrix 1.8 (Vaidya et al. 2011). The COI evolution models were estimated using J-ModelTest 2 (Darriba et al. 2012), the models GTR+G+I, HKY+G, GTR+G were selected for the first, second, and third codons positions, respectively.

The analyses were performed through the CIPRES gateway (Miller et al. 2010) for 5,000,000 generations, with samples taken every 100 generations in 2 parallel analyses and 4 Markov chains. The initial 25% generations were discarded as burn-in. We checked the convergence among the analyses in Tracer 1.7 (Rambaut et al. 2018) checking if the Effective Sample Sizes (ESS) were all > 200. The maximum credibility Bayesian tree was calculated in MrBayes with all compatible groups allowed (contype = allcompat). The branch statistical support was measured by the posterior probability values (PP). Branches with support above 90% are considered strongly supported (Zander 2004). Given current arguments on statistical significance (Amrhein et al., 2019; Hurlbert et al., 2019; Pike, 2019; Wasserstein et al., 2019), the logic, background knowledge, and experimental design should also be evaluated alongside PP to establish a conclusion and determine its certainty. The trees were visualized and edited in FigTree 1.4.3 (Rambaut 2016) and Winclada 1.89 (Nixon 2002), and the final phylogeny was edited in Adobe Illustrator® CS6. Character state reconstructions were based on parsimony and performed in Mesquite 3.8.

2.3. Distribution map

The distributional map was created in QGIS Firenze ver. 3.28 software, using shapefile vector layers from the Instituto Brasileiro de Geografia e Estatística (IBGE) and the Natural Earth (2023) raster data. The Terrestrial Ecosystems of the World layers used in the map are available from the World Wildlife Fund (WWF) (Olson et al. 2001). The distributional records showed in this map came from the examined material in this paper, data available at the Global Biodiversity Information Facility (GBIF), and published literature records (Denning 1951; Denning and Sykora 1966; Flint 1974, 1981; Angrisano and Sganga 2009; Quinteiro and Calor 2012, 2015; Quinteiro and Holzenthal 2017; Henriques-Oliveira et al. 2014, 2018, 2020; Bonfá-Neto et al. 2023, Moura and Quinteiro, 2023). Additional information from distributional records is available as supplementary material (File S2).

3. Results

3.1. Phylogenetic relationship

The maximum credibility Bayesian tree obtained from the morphological characters and COI is presented in Figure 1. To allow the observation of the character-states' distribution on the resulting topology, the characters optimized under delayed transformations (DELTRAN) were displayed along the branches. The combined analysis changed some of the relationship among the species groups presented in the morphological phylogeny of Quinteiro and Almeida (2021), however most of the relationships between species groups have very low statistical support (<50%), reflecting the instability of these conclusions, emphasizing that caution should be used when considering these clades. The resulting tree recovered most species groups as monophyletic. The *inconspicua* and *punctipennis* were strongly supported, but other groups showed moderate (*falicia* group, PP = 76) to weak support (*punctata* group, PP = 61), and very low support (PP<20) to the *avara* and *pratti* groups. The splitting between the *punctipennis* group and other *Oecetis* remained as the first cladogenesis (PP = 98) but with the Austral species *O. inscripta* placed at a distinct lineage from the Neotropical species (PP = 42). In the Austral fauna, *O. inscripta* is placed in a specific group, the *laustra* group, characterized by the absence of any spine or paramere in the phallic apparatus (Wells 2004).

The *avara* group is indicated as monophyletic with very low support (PP = 16). The *punctata* group is placed in a distinct clade (PP = 61) and not within the *avara* group as in Quinteiro and Almeida (2021). The two floating species, *O. rafaeli* and *O. silviae* in the hypothesis of Quinteiro and Almeida (2021), are considered here as sister species (PP = 68). They are placed as a sister group of the *avara* + *punctata* groups (PP = 54).

The cladistic definition of the species groups according with the results are based on the following morphological characters: *avara* group: endotheca small (54:0), forewing fork I sessile (16:1), preanal appendage digitate (28:1) (PP = 16); *inconspicua* group: phallic apparatus asymmetrical (50:1), phallotremal sclerite curved (59:1), phallic apparatus round, inflated (52:1) (PP = 93); *pratti* group: mid leg femur with row of spines (1:1), forewing

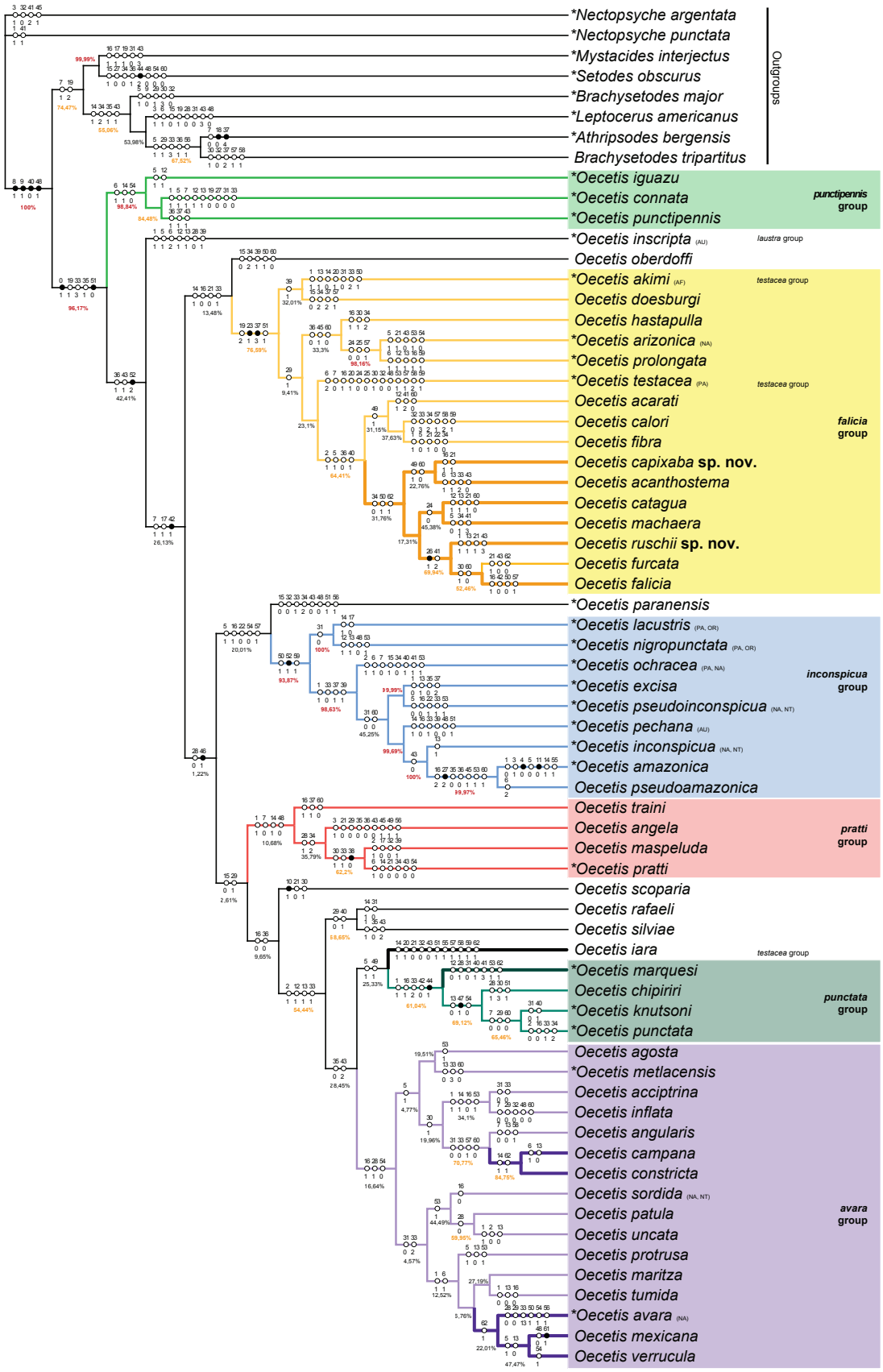

Figure 1. Maximum credibility Bayesian tree obtained from 63 morphological characters and 30 COI sequences coded to *Oecetis* and related taxa (all compatible groups shown). Morphological characters in DELTRAN optimization are displayed along the branches. Black symbols indicate unique character changes. Thick lines indicate lineages with asymmetrical spine projection on the phallotheca. Posterior probability support values are displayed near the node branches, values greater than 50% (majority consensus) are highlighted in orange, strongly supported clades (>90%) are shown in red. Taxa with included COI data are highlighted with *. Non-Neotropical *Oecetis* species distribution are indicated with the following abbreviations: AF Afrotropical, AU Austral, OR Oriental, PA Palearctic, NA Nearctic.

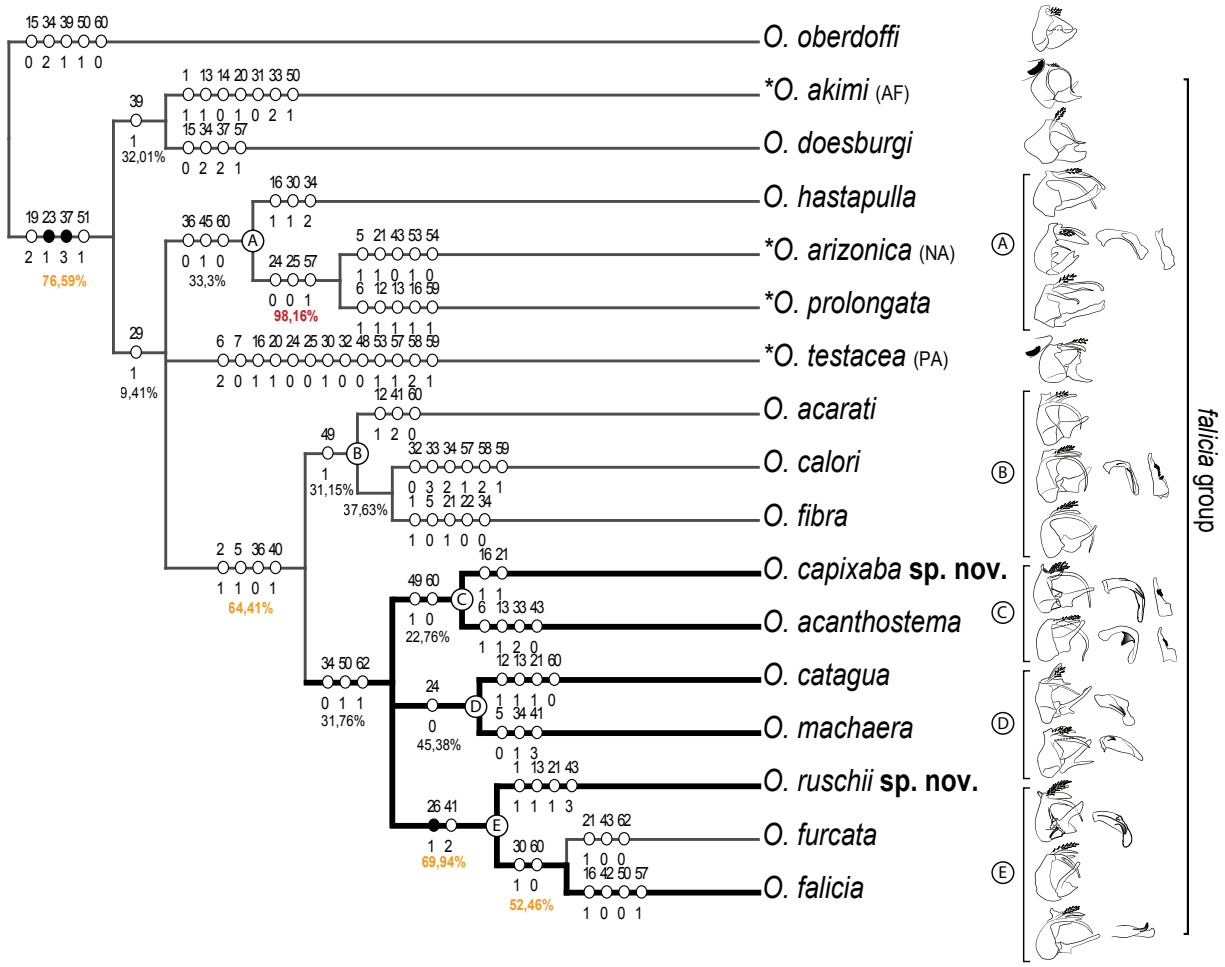

Figure 2. Bayesian tree showing the *Oecetis falicia* group. Morphological characters in DELTRAN optimization are displayed along the branches; clades without supporting morphological characters were collapsed. Black symbols indicate unique character changes. Thick lines indicate lineages with asymmetrical spine projection on the phallotheca. Posterior probability support values are displayed near the node branches, values greater than 50% (majority consensus) are highlighted in orange, strongly supported clades (>90%) are shown in red. Taxa with included COI data are highlighted with *. Non-Neotropical *Oecetis* species distribution are indicated with the following abbreviations: AF Afrotropical, PA Palearctic, NA Nearctic. Illustrations of the male genitalia in lateral view based on original descriptions are depicted next to each species label, showing also for some species the lateral view of the phallic apparatus and the ventral view of the inferior appendage.

sectorial crossvein aligned (7:0), forewing apex acuminate (14:1), segment IX posterolateral margin setae absent (48:0) (PP = 10); *punctata* group: mid leg femur with row of spines (1:1), forewing fork I sessile (16:1), tergum X with irregular shape (33:2), inferior appendage ventral lobe small (42:0), inferior appendage quadrate, with thick setae (44:1) (PP = 61); *punctipennis* group: forewing fork V sessile (6:1), forewing apex acuminate (14:1), endotheca small (54:0) (PP = 98); *falicia* group: presence of dorsolateral process on the segment IX (23:1), tergum IX shorter than sternum IX (19:2), inferior appendage dorsal lobe triangular (37:3), and phallic apparatus elongate (51:1) (PP = 77).

Focusing on the *falicia* group (Fig. 2), the first cladogenesis shows a clade with *Oecetis doesburgi* and the afrotropical *Oecetis akimi* being the first to include typical characters of the group. The analysis shows a clade with North American, Central American and northern South American species (clade A), (*O. hastapulla* (*O. arizonica*, *O. prolongata*) (PP = 33), on which the most conspicuous synapomorphy is the inferior appendage distal lobe with apical incision (45:1). Within this clade, *O. arizonica* from southern USA and *O. prolongata* from Costa Rica are shown as strongly supported sister species (PP = 98). *Oecetis testacea*, from Europe and East Asia, was recovered as an independent and very autapomorphic lineage. The result also show a clade (PP = 64) formed by species primarily from the Atlantic Forest and some from Amazon and Central America, presenting an inferior appendage with ventral lobe (40:1), but without the dorsal lobe (36:0), foreleg tibia with apical spur (5:1) and midleg femur spines covering half podomere (2:1). The first cladogenesis of this clade are of species that do not have an asymmetric spine, i.e. the clade B (*O. acarati* (*O. calori*, *O. fibra*)) (PP = 31). The asymmetric spine on the phalloteca (62:1) appeared once among the analyzed species of the *falicia* group and defines what may be considered as an unresolved clade ((*O. catagua*, *O. machaera*), (*O. capixaba* **sp. nov.**, *O. acanthostema*), (*O. ruschii* (*O. furcata*, *O. falicia*))) (PP = 31). The clade C, *O. capi-*

xaba **sp. nov.**, is grouped as sister of *O. acanthostema* (PP = 40) based on the characters: inferior appendage with spine-like setae (49:1), and phallotremal sclerite absent (60:0). The clade D, *O. catagua* and *O. machaera*, share the character dorsolateral process of segment IX straight (24:0) (PP = 45). *Oecetis ruschii* **sp. nov.** forms a clade with *O. furcata* + *O. falicia* (PP = 69) (clade E), which is based on the synapomorphies: dorsolateral process of segment IX forked (26:1), and inferior appendage ventral lobe triangular (41:2).

3.2. Taxonomy

LEPTOCERIDAE Leach, 1815

Oecetis McLachlan, 1877

Oecetis capixaba sp. nov.

https://zoobank.org/8DC22D91-23E7-4751-ADAC-C4A-7C67AFF56

Figure 3A–F

Type material. Holotype: BRAZIL • ♂; Espírito Santo, Santa Teresa, Augusto Ruschi biological reserve, Córrego Roda d'Água; 19°53′35.1″S, 40°32′39.7″W; 810 m a.s.l.; 24 Aug. – 30 Sep. 2017; Malaise trap; FF Salles, V Costa, P Bonfá Nt leg.; UFVB TR00336.

Diagnosis. This new species is similar to the other species of the *falicia* group with spine-like setae on the inner surface of the inferior appendage, being very similar to *Oecetis achanthostema* by both presenting a spiny process on the phalloteca. They can be differentiated by the dorsolateral process of segment IX in dorsal view being wide subapically in *O. achanthostema*, while it is tapered and overall narrow in the new species. The spine-like setae on the inferior appendage are conspicuously longer in the new species than in *O. achanthostema*. Additionally, the phallic apparatus of *O. achanthostema* has two digitate apical projections, which are absent in *O. capixaba* **sp. nov.**

Description. Adult male: Forewing length 6.8 mm (n = 1). *Head.* Color pale light yellow (in alcohol). Antennae approximately 3x forewing length; scape stout, elongate; pedicel enlarged in width, narrower than scape, shorter than first flagellomeres; first flagellomere narrow, with same length as scape, other flagellomeres shorter than first. Maxillary palps pale light yellow, 5-segmented, segments subequal in length and width, densely covered with setae. Labial palps pale light yellow, apparently 4-segmented, first segment very small. *Thorax.* Pterothorax yellowish brown; forewing pale light yellow; dark bands over cord absent (Fig. 3A); dark spots absent; forks I sessile and fork V rooted (Fig. 3A); sectoral crossvein (s) not aligned with r–m (Fig. 3A). Hind wing with forks I and V present (Fig. 3B); false vein near Cu1a (Fig. 3B). Legs pale yellow brown, mid leg with longitudinal row of spines on tibia and tarsal segments. Tibial spur formula 1,2,2, fore tibial spur small. *Genitalia* (Fig. 3C–F). Segment IX in lateral view annular, short, bearing pair of dorsolateral processes; processes slender, bent ventrad, cylindrical, tapering posteriorly, same length as phallic apparatus; two acrotergite present dorsolaterally (Fig. 3C, D). Preanal appendage short and narrow, digitate, setose (Fig. 3C, D). Tergum X, in lateral view, divided into dorsal and ventral lobes; dorsal lobe, single, cylindrical, digitate, slightly larger than the length of the ventral lobe, with short apical setae (Fig. 3C, D); ventral lobe divided mesally by V-shaped incision, forming two lobes, each broad basally, tapering to acuminate apex (Fig. 3C, D). Inferior appendage 1-segmented, broad at base, setose; distal lobe long, narrow, tapering posteriorly, apex rounded, with short, stout spine-like setae present on inner surface (Fig. 3D, E); ventral lobe, in lateral view, quadrate (Fig. 3C, E); dorsal lobe reduced (Fig. 3D). Phallic apparatus bilaterally asymmetrical, bent ventrad, cylindrical, elongate, membranous apically, with posterolateral spine projection on right side (Fig. 3F–H); apex elongate, in caudal view (Fig. 3H); phallic spines absent (Fig. 3F, G); phallotremal sclerite absent (Fig. 3G).

Etymology. The specific epithet "capixaba" is a name originating from the Tupi language, meaning "farmland", "a land clean for planting", and it is currently used to designate people born in the state of Espírito Santo. Species named in apposition.

Oecetis ruschii sp. nov.

http://zoobank.org/A32DF25F-0A75-4259-9EDB-56F33C6A3ED3

Figure 4A–F

Type material. Holotype: BRAZIL • ♂; Espírito Santo, Santa Teresa, Augusto Ruschi biological reserve, Córrego Roda d'Água; 19°53′35.1″S, 40°32′39.7″W; 810 m a.s.l., 21–22 Oct. 2017; light pan trap; FF Salles, V Costa, P Bonfá Nt leg.; UFVB TR00337. **Paratypes.** BRAZIL • 1♂; same data as holotype; UFVB TR00338; • 1♂; same data, except 28 Dec. 2017; UFVB TR00339; • 1♂; same data, except 17 Jan. – 20 Feb. 2018; Malaise trap; UFVB TR00340; • 1♂; same data, except 20–21 Feb. 2018; UFVB TR00341.

Diagnosis. This species is similar to *Oecetis furcata* and *O. falicia*, all species presenting a bifurcation in the dorsolateral process of segment IX. *Oecetis ruschii* **sp. nov.** can be differentiated by the dorsolateral process of segment IX having a long ventrolateral bifurcation and a short dorsal subapical one, in *O. furcata* there is a single ventral bifurcation, and in *O. falicia* it is dorsal and short. The inferior appendage distal lobe in the new species is wider in lateral view than in *O. furcata* and *O.*

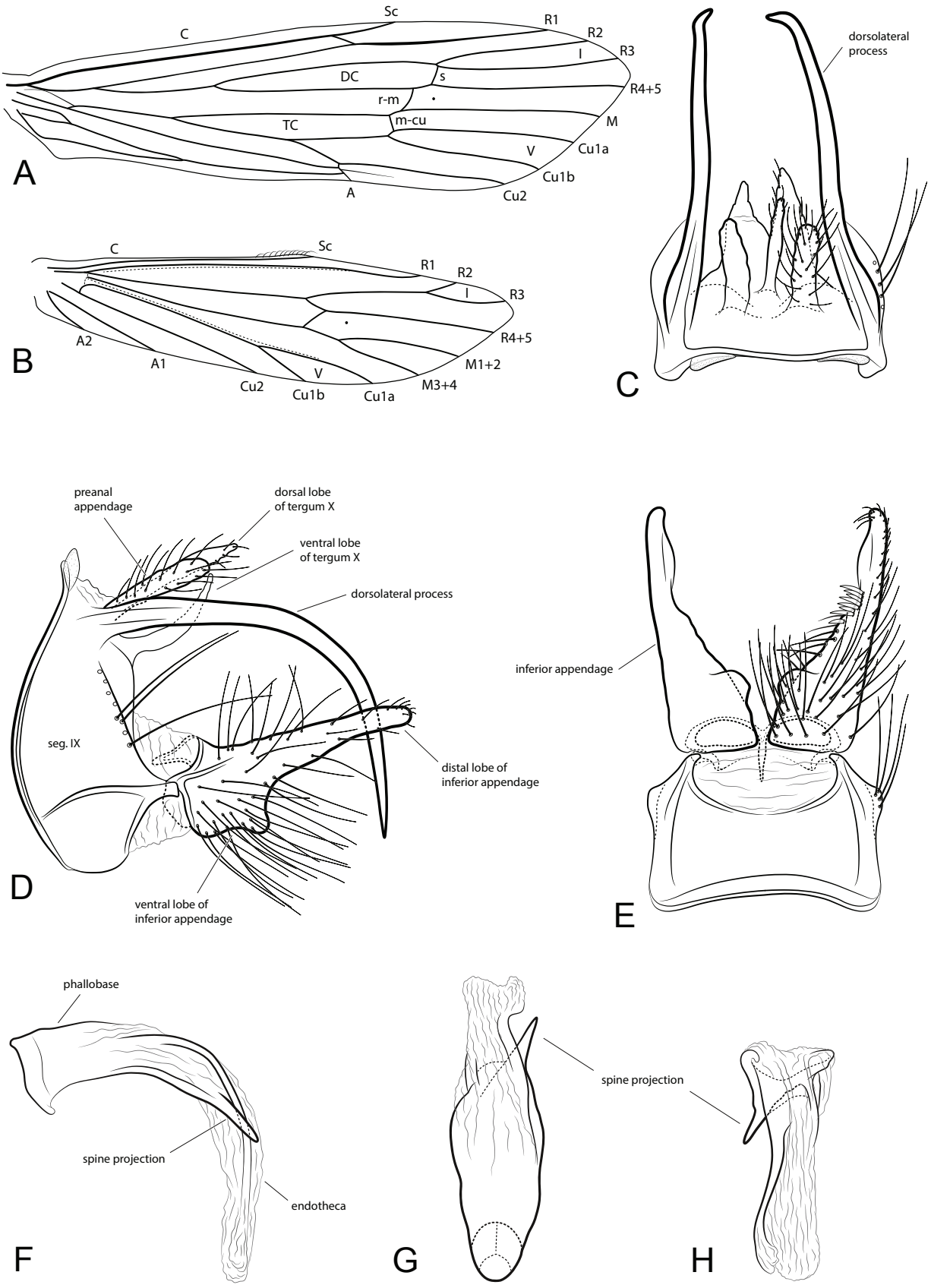

Figure 3. *Oecetis capixaba* **sp. nov.**, holotype, male (UFVB TR00336). Venation: **A** forewing, **B** hind wing. Genitalia: **C** dorsal, **D** right lateral, **E** ventral. Phallus: **F** right lateral, **G** dorsal, **H** caudal.

falicia. The apex of this lobe in ventral view is triangular, wide, and flat in the new species while it is regular and digitate in the other species. Additionally, the new species has an asymmetrical projection on the phallic apparatus that is also present in *O. falicia* but absent in *O. furcata*.

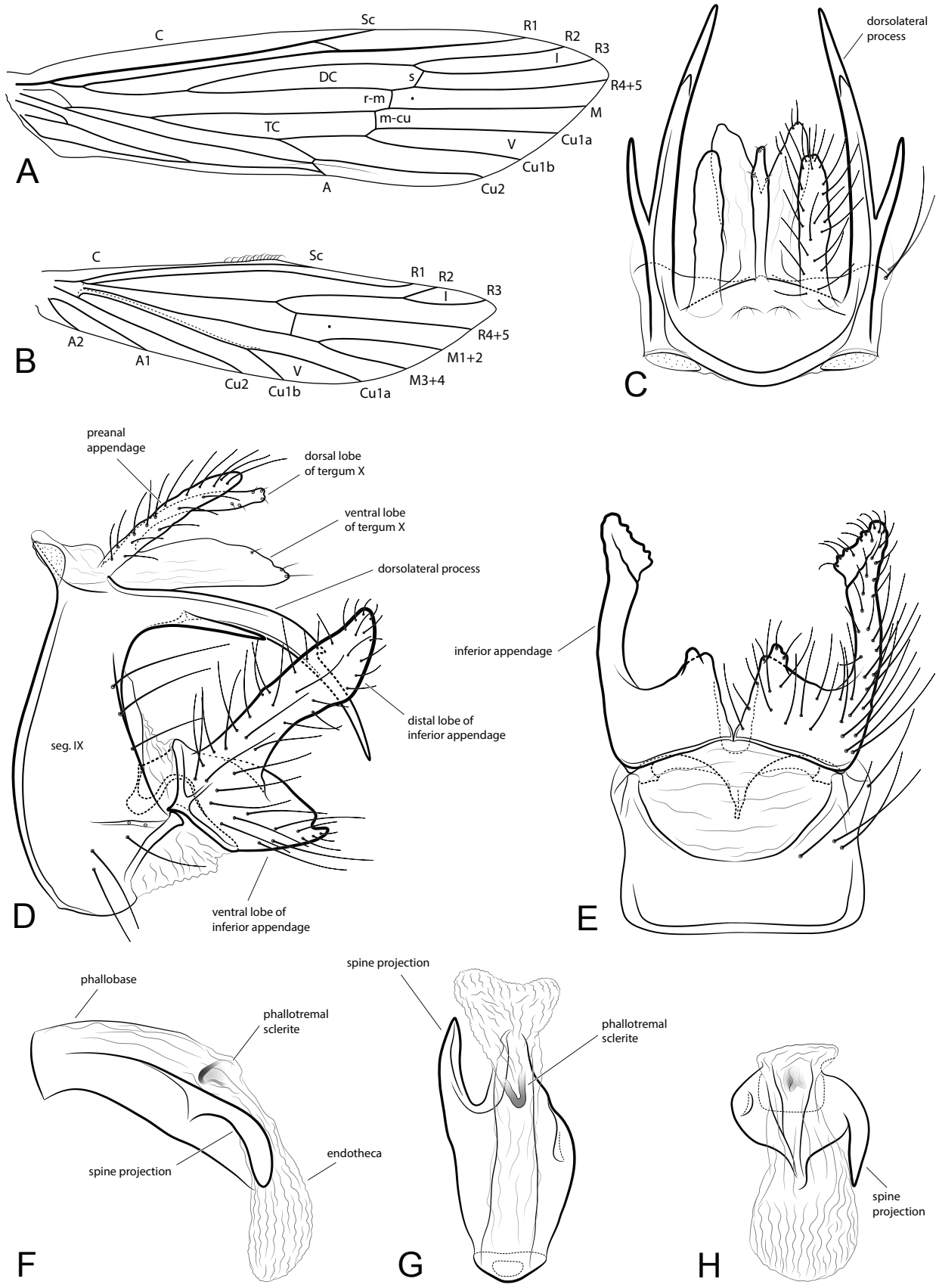

Figure 4. *Oecetis ruschii* **sp. nov.**, holotype, male (UFVB TR00337). Venation: **A** forewing, **B** hind wing. Genitalia: **C** dorsal, **D** left lateral, **E** ventral. Phallus, **F** left lateral, **G** dorsal, H caudal.

Description. Adult male: Forewing length 6.2–7.1 mm (n = 5). — *Head*. Color yellowish brown (in alcohol). Antennae approximately 3x forewing length; scape stout, elongate; pedicel enlarged in width, narrower than scape, shorter than first flagellomeres; first flagellomere narrow, with same length as scape, other flagellomeres shorter

than first. Maxillary palps yellowish brown, 5-segmented, segments subequal in length and width, densely covered with setae. Labial palps yellow, apparently 4-segmented, first segment very small. — *Thorax*. Pterothorax yellowish brown; forewings yellowish brown; dark bands over cord present; dark spots absent; forks I and V rooted (Fig. 4A); sectoral crossvein (s) not aligned with r–m (Fig. 4A). Hind wing forks I and V present; false vein near Cu1a (Fig. 4B). Legs pale yellowish brown, mid legs with row of small spines on tibia and tarsus, and hind legs with row of small spines on the tarsus. Tibial spur formula 1,2,2, fore tibial spur small. *Genitalia* (Fig. 4C–F). Segment IX annular and short; dorsolateral process present, long and bilobed, ventrolateral lobe 1/3x main lobe length, with apex acute; main lobe dorsally with short subapical spine-like lobe, apex acute; two acrotergite present dorsolaterally (Fig. 4C, D). Preanal appendage long and narrow, digitate, setose (Fig. 4C). Tergum X in lateral view, divided into dorsal and ventral lobes; dorsal lobe single, cylindrical, slightly enlarged subapically, digitate, slightly shorter than the length of the ventral lobe, with short apical setae (Fig. 4C); ventral lobe in dorsal view, divided mesally by V-shaped incision, forming two lobes, broad basally, tapering apically (Fig. 4C); in lateral view broad. Inferior appendage 1-segmented, broad at base, setose; distal lobe long, cylindrical, apex triangular, with mesal projection in ventral view (Fig. 4E); ventral lobe broad, trapezoid in lateral view (Fig. 4D); quadrate with small hump on mid inner portion in ventral view (Fig. 4E); dorsal lobe reduced (Fig. 4D). Phallic apparatus asymmetrical, narrow basally, broad mesally, bent ventrad, with posterolateral spine projection on left side, apex membranous (Fig. 4F); endotheca longer than phallobase (Fig. 4F, G); phallic spines absent (Fig. 4F, G); phallotremal sclerite present (Fig. 4G).

Etymology. The specific epithet is the name of the biological reserve where the specimens were collected, which was named in honor of the naturalist and environmental activist Augusto Ruschi.

3.3. New Records

In this section we present new distributional records for *Oecetis* species in Brazil, new records for the country's states are shown in bold.

Oecetis connata Flint, 1974

Material analyzed. BRAZIL • 1♀, 5♂♂; Espírito Santo, Linhares, Lagoa Juparanã Mirim (Lagoa Nova); 19°19′49.0″S, 40°10′12.3″W; 12–13 Sep. 2022; Pennsylvania Light Trap; ADL Viana, P Bonfá Nt, AD Ataíde leg.; UFVB TR00856; • 1♂; Minas Gerais, Conceição do Mato Dentro, Cânion do Peixe Tolo; 19°00′15.0″S, 43°36′39.0″W; 01 Dec. 2020, light over white cloth, FF Salles leg.; UFVB TR00857.

Distribution. Brazil (Acre, Amazonas, Pará, Bahia, Piauí, Mato Grosso, Rio de Janeiro, São Paulo, **Espírito Santo**, **Minas Gerais**), Guiana, Suriname.

Oecetis flinti Quinteiro & Holzenthal, 2017

Material examined. BRAZIL • 1♀, 1♂; Minas Gerais, Conceição do Mato Dentro, Cânion do Peixe Tolo; 19°00′15.0″S, 43°36′39.0″W; 01 Dec. 2020; light over white cloth; FF Salles leg.; UFVB TR00858.

Distribution. Brazil (**Minas Gerais**, Tocantins)

Oecetis inconspicua (Walker, 1852)

Material examined. BRAZIL, • 31♀♀, 1♂; Espírito Santo, Linhares, Lagoa Juparanã Mirin (Lagoa Nova); 19°19′49.0″S, 40°10′12.3″W; 12–13 Sep. 2022; Pennsylvania Light Trap; ADL Viana, P Bonfá Nt, AD Ataíde leg. UFVB TR00859; • 1♂; Espírito Santo, Linhares, São Rafael, cachoeira de Angeli; 19°20′55.6″S, 40°25′17.9″W; 25 Sep. 2020; light over white cloth; FF Salles, P Bonfá Nt, TS Raymundo, DS Ferreira leg.; UFVB TR00860.

Distribution. Bahamas, Brazil (Amazonas, Bahia, Paraíba, Pernambuco, Piauí, Mato Grosso, Minas Gerais, Rio de Janeiro, São Paulo, **Espírito Santo**, Paraná, Santa Catarina), Canada, Colombia, Costa Rica, Cuba, El Salvador,United States, Guatemala, Honduras, Jamaica, Mexico, Nicaragua, Panama, Peru, Puerto Rico, Venezuela.

Oecetis paranensis Flint, 1982

Material examined. BRAZIL• 1♂; Espírito Santo, Linhares, São Rafael, cachoeira de Angeli; 19°20′55.6″S, 40°25′17.9″W; 25 Sep. 2020; light over white cloth; FF Salles, P Bonfá Nt, TS Raymundo, DS Ferreira leg.; UFVB TR00861.

Distribution. Argentina, Brazil (Amazonas, Bahia, Pernambuco, Mato Grosso do Sul, Minas Gerais, São Paulo, **Espírito Santo**), Paraguay, Peru.

4. Discussion

Better supported clades within the *falicia* group are the Nearctic and Central America species (*O. arizonica* + *O. prolongata*), the large clade including most South American species with inferior appendage presenting ventral lobe but without dorsal lobe (clades B, C, D, and E), and the clade E formed by species with forked dorsolateral process of segment IX. Most other clades showed low statistical support, suggesting that they can change significantly as more specimens and characters are included in the analysis. The species of the included *testacea* group (*O. akimi*, *O. testacea*, and *O. iara*) have long autapomorphic branches that might indicate phylogenetic noise. As suggested by Quinteiro and Almeida (2021), more representatives of the *testacea* group would be necessary to clarify its phylogenetic position. A great part of the included *falicia* group species have no molecular data available so far. Therefore, many inferred relationships

relied only on morphology. Groups for which both morphology and COI data are largely available for the terminal taxa (*inconspicua*, *punctipennis*, *punctata* groups) in general showed clades with stronger supports. Despite genomic data now being increasingly used to infer phylogenetic relationships, this kind of data is just available for very few species. The great majority of the world's species do not have a single molecular marker available. On the other hand, morphology is intrinsically incorporated in the species description process, therefore it is largely available, inexpensive, and also has a more straightforward association with the specimen biology. However, the number of morphological characters is comparatively smaller and the characters are rather complex than the nucleotides sequences. Making use of the reciprocal illumination (Hennig 1950, 1966), the combination of the morphology and the available gene fragments may help indicating relationships unnoticed through the morphological assessment only, at the same time that the morphology helps signaling relevant phenotypic traits, and reducing the molecular bias of the gene history and misleading fast evolving regions. This approach therefore provides a stronger hypothesis.

4.1. Distribution and biogeography

The distribution of the species in clade A suggests that this clade is widespread from southern USA, Central America, and northern South America (Fig. 5 dot 3, 11 and 13). In the clade B, *O. acarati* is known from the southern Atlantic Forest (Argentina) and *O. calori* Quinteiro & Holzenthal 2017 from central Atlantic Forest (Brazil, Minas Gerais state) (Fig. 5 dot 2 and 4); *O. fibra* is widespread from the south to the central Atlantic Forest (Fig. 5 dot 9). On clade C, *O. acanthostema* is from northeastern Brazil Cerrado ecoregion and *O. capixaba* **sp. nov.** from the Atlantic Forest (Brazil, Espírito Santo state) (Fig. 5 dot 1 and 5). For the clade D, *O. catagua* is from Cerrado and Atlantic Forest ecoregion (Brazil, Minas Gerais and Espírito Santo state) and *O. machaera* from Amazon forest (Brazil, Amazon state) (Fig. 5 dot 6 and 12). While for clade E, *Oecetis ruschii* **sp. nov.**, and *O. furcata* have a close distribution both in northern Atlantic Forest (Bahia and Espírito Santo states in Brazil) (Fig. 5 dot 10 and 14), and *O. falicia* occurs in Central America (Panama) (Fig. 5 dot 8). This disjunct distribution between *Oecetis falicia*, *O. ruschii* **sp. nov.**, and *O. furcata* suggests the possible existence of additional undescribed species within this lineage or a wider distribution range of the known species.

The historical connections between the Atlantic and Amazon Forests with their expansion over the dry vegetation (Cerrado ecoregion) has been advocated as a general hypothesis to the explanation of disjunct distributions of lineages inhabiting the two ecoregions, with an older connection occurring through a southern route during the Miocene, and a more recent connection in a route through the Northeast Region during the Pliocene and Pleistocene and associated with the Quaternary climate changes (Batalha-Filho et al. 2013; Ledo and Colli 2017). The cladogenesis between *Oecetis catagua* (from the Cerrado ecoregion) and *O. machaera* (from the Amazon Forest ecoregion), and the relationship of *O. facilia* (from Panama), *Oecetis ruschii* **sp. nov.** and *O. furcata* (from the Atlantic Forest ecoregion), may be explained by these ancient connections between the Atlantic and Amazon Forests, however, the limited information about species distribution (which is mostly from type locality only), and the unknown divergence times (which can be much older or much recent) restrict our conclusions about the biogeographical history of these species.

4.2. Asymmetric genitalia

The asymmetric spiny process on the phallotheca is indicated to appear a single time within the *falicia* group and lost in *O. furcata*. An asymmetrical process evolved several times in different species groups as it is present also in the *avara* and *punctata* groups. The asymmetry in the phallic apparatus is also a synapomorphy of the *inconspicua* group, although the asymmetry in this group is not associated with the presence of a spiny process, but on the overall shape of the phallic apparatus.

Huber et al. (2007) provide a review of asymmetrical genitalia for several insect groups, including Trichoptera. Asymmetrical genitalia are reported in the major Trichoptera subgroups and evolved multiple times convergently. The occurrence of asymmetric and symmetric individuals in a same species is also reported for *Phylloicus* Müller, 1880 (Prather 2003). Asymmetry in females with few exceptions is mostly not mentioned (Huber et al. 2007). *Oecetis catagua* has the asymmetric process on the phallic apparatus, and in the respective female there is no indication of asymmetry in the genitalia (Henriques-Oliveira et al. 2018). In insects, it seems that male asymmetries tend to evolve first, and female asymmetries evolve later, if they ever occur (Huber et al. 2007). Male position with torsion during copula is advocated as the most important aspect to explain insect genital asymmetry (Huber et al. 2007). However, there is not much detailed information about copulatory positions in Trichoptera. What is available suggests a final end-to-end position (Malicky 1973; Erman 1984) and no twist of the abdomen or even the phallus (Tobias 1972; Statzner 1974). Therefore, to better understand the role of *Oecetis* genitalia asymmetry, more in-depth research on copula and the functional interaction between the male and female genitalia is required.

5. Conclusion

In this study, we included additional available molecular evidence to the morphologic phylogenetic estimations of the Neotropical *Oecetis* and a larger sample of Neotropical representatives of the *falicia* group, including two new species from Atlantic Forest. The main conclusions are:

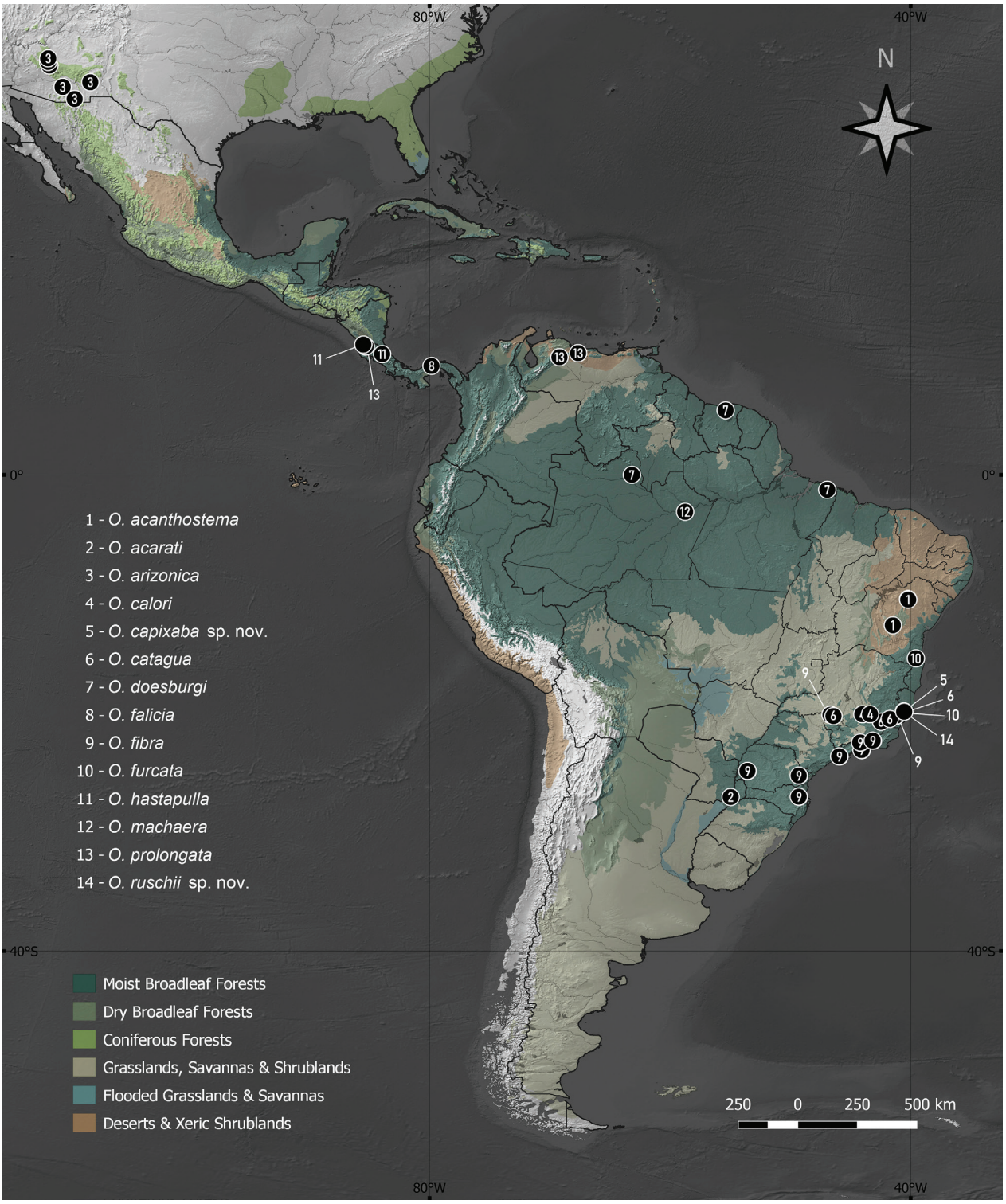

Figure 5. Distribution map of Neotropical species in the *falicia* group.

(**1**) Most species groups were recovered as monophyletic, however the *punctata*, *pratti* and *avara* groups had low to extremely low supports. In Quinteiro and Almeida (2021) the *avara* group was recovered as paraphyletic due to the placement of the *punctata* group within it, but also with a very low support. Given the poor support for phylogenetic relationships presented by Quinteiro & Almeida (2021) and in this study, the phylogenetic relationships within *Oecetis* should be considered preliminary and their interpretation treated with caution. Further research, e.g. based on morphology and multi-locus molecular data, is still necessary to clarify these and other issues of the *Oecetis* species relationships.

(**2**) The two new species from the *falicia* group herein described have an asymmetric spiny projection on the phalloteca, which was indicated to have evolved a single time in this species group and lost in the *O. furcata*. Asymmetrical phallic projections also evolved independently in the *avara* and *punctata* group.

(**3**) Most of the *falicia* group species that share this character occur primarily near the Atlantic coast of South America on the Atlantic Forest and Cerrado ecoregions. A single species is known from the Amazon Forest, and a very disjunct species, *O. falicia*, is known from Central America. The large gap between *O. falicia* and related taxa from the Atlantic Forest suggest the existence of undescribed species in this lineage or a wider distribution range of the known species.

(**4**) The function of the asymmetric spine on male genitalia remains uncertain, and it is not associated with any conspicuous asymmetry in the female internal genitalia. This lack of asymmetry in females supports Huber et al. (2007) conclusion that in insects male asymmetry often evolves prior to female asymmetry.

6. Data availability

The data underlying this article, including the resulting tree (.tre), the morphological (.ss) and the COI matrix (.fas), as well as the combined matrix used in the Bayesian analysis (.nex) are available at the Open Science Framework (OSF) repository and can be accessed at https://osf.io/cp56j/?view_only = b431ca26c7d94ffa9a0ed08376c1cccd

7. Acknowledgements

This study was financially supported by the Conselho Nacional de Desenvolvimento Científico (CNPq, grant process 309666/2019–8) and Fundação de Amparo à Pesquisa e Inovação do Espírito Santo (FAPES, grant process 60016604/12; 61938408/13) to FFS; Coordenação de Aperfeiçoamento de Pessoal de Nível Superior – Brasil (CAPES) – Finance Code 001 (006/2022 PROPG-PDEE) to AV; and (CAPES) – Finance Code 001 (process 88887.899774/2023-00) to PBN.

We are grateful to the members of the Laboratory of Systematics and Ecology of Insects (LabSEI, UFES) and the Museu de Entomologia UFV who contributed to collections and field trips. We thank the reviewers and editor for reading and commenting on our manuscript.

8. References

Amrhein V, Greenland S, McShane B (2019) Scientists rise up against statistical significance. Nature 567: 305–307. https://doi.org/10.1038/d41586-019-00857-9

Angrisano EB, Sganga JV (2009) Two new species of Trichoptera from Salto Encantado Provincial Park (Misiones Province, Argentina). Aquatic Insects 31(4): 271–278. http://dx.doi.org/10.1080/01650420903113729

Banks N (1895) New neuropteroid insects. Transactions of the American Entomological Society 22: 313–316.

Batalha-Filho H, Fjeldså J, Fabre PH, Miyaki CY (2013) Connections between the Atlantic and the Amazonian forest avifaunas represent distinct historical events. Journal of Ornithology 154: 41–50. http://dx.doi.org/10.1007/s10336-012-0866-7

Blahnik RJ, Holzenthal RW (2014) Review and redescription of species in the *Oecetis avara* group, with the description of 15 new species (Trichoptera, Leptoceridae). ZooKeys 376: 1–83. https://doi.org/10.3897/zookeys.376.6047

Blahnik RJ, Holzenthal RW, Prather AL (2007) The lactic acid method for clearing Trichoptera genitalia. In: BuenoSoria J, Barba-Álvarez R, Armitage B (Eds) Proceedings of the 12th International Symposium on Trichoptera. Columbus, The Caddis Press, 9–14.

Bonfá-Neto P, Vilarino A, Salles FF (2023) Breviteritoria Weaver 1984 (Trichoptera: Integripalpia) of Espírito Santo State, Brazil: New records and new species. Zootaxa 5336(3): 301–327. https://doi.org/10.11646/zootaxa.5336.3.1

Chen YE (1993) Revision of the *Oecetis* (Trichoptera: Leptoceridae) of the World. Clemson University, unpublished PhD dissertation.

Darriba D, Taboada G, Doallo R, Posada D (2012) jModelTest 2: more models, new heuristics and parallel computing. Nature Methods 9: 772. https://doi.org/10.1038/nmeth.2109

Denning DG (1951) Records and descriptions of Nearctic caddis flies. Part III. Journal of the Kansas Entomological Society 24: 157–162. http://www.jstor.org/stable/25081981

Denning DG, Sykora JL (1966) New North American Trichoptera. Canadian Entomologist 98: 1219–1226. https://doi.org/10.4039/Ent981219-11

Erman NA (1984) The mating behavior of *Parthina linea* (Odontoceridae), a caddisfly of springs and seeps. In: Morse JC (Ed.) Proceedings of the Fourth International Symposium on Trichoptera. Dr. W. Junk, The Hague, Netherlands, 131–136.

Flint OS (1974) The Trichoptera of Surinam. Studies of Neotropical caddisflies, XV. Studies on the Fauna Suriname and other Guyanas 14: 1–151.

Flint OS (1981) Studies of Neotropical caddisflies, XXVIII: The Trichoptera of the Río Limón Basin, Venezuela. Smithsonian Contributions to Zoology 330: 1–61. https://doi.org/10.5479/si.00810282.330

Flint OS (1982) Studies of neotropical caddisflies. XXXI. Five new species from Argentina (Trichoptera). Entomol. News 93: 43–97.

Goloboff PA, Morales ME (2023) TNT version 1.6, with a graphical interface for MacOS and Linux, including new routines in parallel. Cladistics 39(2): 144–153. https://doi.org/10.1111/cla.12524

Hennig W (1950) Grundzüge einer Theorie der phylogenetischen Systematik Deutscher Zentralverlag, Berlin, 370 pp.

Hennig W (1966) Phylogenetic Systematics University of Illinois Press, Urbana, Chicago, London, 263 pp.

Henriques-Oliveira AL, Dumas LL, Nessimian JL (2014) Three new species and new distributional records of *Oecetis* McLachlan 1877 (Trichoptera: Leptoceridae: Leptocerinae) from Brazil. Zootaxa 3753: 273–282. https://doi.org/10.11646/zootaxa.3753.3.6

Henriques-Oliveira AL, Rocha IC, Nessimian JL (2018) Leptoceridae (Insecta, Trichoptera) from Serra da Canastra Mountain Range, Southeast Brazil: Diversity, Distribution, and Description of Two New Species. Neotrop Entomol 48: 277–289. https://doi.org/10.1007/s13744-018-0633-4

Henriques-Oliveira AL, Dumas LL, Nessimian JL (2020) Leptoceroidea (Insecta: Trichoptera: Integripalpia) from Serra do Caparaó, Southeast Brazil, including a new species of Atanatolica Mosely (Leptoceridae). Zootaxa 4763(1): 31–49. https://doi.org/10.11646/zootaxa.4763.1.3

Huber BA, Sinclair BJ, Schmitt M (2007) The evolution of asymmetric genitalia in spiders and insects. Biological Reviews 82: 647–698. https://doi.org/10.1111/j.1469-185X.2007.00029.x

Hurlbert SH, Levine RA, Utts J (2019) Coup de grâce for a tough old bull:"Statistically significant" expires. The American Statistician 73: 352–357. https://doi.org/10.1080/00031305.2018.1543616

Jell PA, Duncan PM (1986) Invertebrates, mainly insects, from the freshwater, Lower Cretaceous, Koonwarra fossil bed (Korumburra group), South Gippsland, Victoria. Memoirs of the Association of Australasian Palaeontologists 3: 111–205.

Johanson KA, Mary NJ, Sjöberg T, Malm T (2020a) Eighteen new species of *Oecetis* McLachlan 1877 (Trichoptera, Leptoceridae) from New Caledonia. Zootaxa 4809(2): 201–240. https://doi.org/10.11646/zootaxa.4809.2.1

Johanson KA, Pham TH, Malm T, Sjöberg T (2020b) Description of six new species of *Oecetis* (Trichoptera, Leptoceridae) from Vietnam. Zootaxa 4816(3): 311–324. https://doi.org/10.11646/zootaxa.4816.3.2

Katoh K, Standley DM (2013) MAFFT multiple sequence alignment software v.7: improvements in performance and usability. Molecular Biology and Evolution 30: 772–780. https://doi.org/10.1093/molbev/mst010

Leach WE (1815) Entomology. In: Brewster D (Ed.) The Edinburgh encyclopedia. William Blackwood, Edinburgh, 52–172.

Ledo RMD, Colli GR (2017) The historical connections between the Amazon and the Atlantic Forest revisited. Journal of Biogeography 44(11): 2551–2563. https://doi.org/10.1111/jbi.13049

Lewis PO (2001) A likelihood approach to estimating phylogeny from discrete morphological character data. Systematic Biology 50: 913–925. https://doi.org/10.1080/106351501753462876

Maddison WP, Maddison DR (2023) Mesquite: a modular system for evolutionary analysis. Version 3.81 http://www.mesquiteproject.org

Malicky H (1973) Trichoptera (Köcherfliegen). Handbuch der Zoologie, IV. Arthropoda, 2. Insecta 29: 1–114.

Malicky H (2005) Beiträge zur Kenntnis asiatischer *Oecetis* (Trichoptera, Leptoceridae). Linzer Biologische Beiträge 37: 605–669.

Malm T, Johanson KA (2011) A new classification of the long-horned caddisflies (Trichoptera: Leptoceridae) based on molecular data. BMC Evolutionary Biology 11(10): 1–17. https://doi.org/10.1186/1471-2148-11-10

Malm T, Johanson KA, Wahlberg N (2013) The evolutionary history of Trichoptera (Insecta): A case of successful adaptation to life in freshwater. Systematic Entomology 38(3): 459–473. https://doi.org/10.1111/syen.12016

McLachlan R (1877) A Monographic Revision and Synopsis of the Trichoptera of the European Fauna (1874–1880). London: John van Voorst. https://doi.org/10.5962/bhl.title.28556

Miller MA, Pfeiffer W, Schwartz T (2010) Creating the CIPRES Science Gateway for inference of large phylogenetic trees. In: Proceedings of the Gateway Computing Environments Workshop. New Orleans, 1–8. https://doi.org/10.1109/GCE.2010.5676129

Milne LJ (1934) Studies in North American Trichoptera. Part 1. Cambridge, Massachusetts, 1–19 pp.

Morse J (2023) Trichoptera World Checklist. URL. https://trichopt.app.clemson.edu/welcome.php (accessed Sept. 2023).

Moura L, Quinteiro FB (2023) Diversity of Leptoceroidea (Insecta: Trichoptera) in Par State, Brazil: A new species of *Oecetis* McLachlan 1877 and new records. Zootaxa 5361(4): 555–565. https://doi.org/10.11646/zootaxa.5361.4.5

Müller F (1880) Sobre as casas construidas pelas larvas de insectos Trichopteros da Provincia de Santa Catharina. Archivos do Museu Nacional do Rio de Janeiro III: 99–134, 210–215, 134 plates.

Natural Earth (2023) Free vector and raster map data. Available at: http://naturalearthdata.com (accessed Sept. 2023).

Neboiss A (1989) The *Oecetis reticulata* species-group from the South-West Pacific area (Trichoptera: Leptoceridae). Bijdragen tot de Dierkunde 59: 191–202. https://doi.org/10.1163/26660644-05904001

Nixon KC (2002) WinClada, v.1.00.08. Ithaca: Published by the author. Available at: http://www.diversityoflife.org/winclada (accessed Sept 2023).

Olson DM, Dinerstein E, Wikramanayake ED, Burgess ND, Powell GVN, Underwood EC, D'Amico JA, Itoua I, Strand HE, Morrison JC, Loucks CJ, Allnutt TF, Ricketts TH, Kura Y, Lamoreux JF, Wettengel WW, Hedao P, Kassem KR (2001) Terrestrial ecoregions of the world: a new map of life on earth: a new global map of terrestrial ecoregions provides an innovative tool for conserving biodiversity. Bioscience 51(11): 933–938. https://doi.org/10.1641/0006-3568(2001)051[0933:TEOTWA]2.0.CO;2

Pike H (2019) It's time to talk about ditching statistical significance. Nature 567: 283. https://doi.org/10.1038/d41586-019-00874-8

Prather AL (2003) Revision of the neotropical caddisfly genus *Phylloicus* (Trichoptera: Calamoceratidae) Zootaxa 275: 1–214. https://doi.org/10.11646/zootaxa.275.1.1

Quinteiro FB, Almeida EAB (2021) Systematics of Neotropical *Oecetis* McLachlan, 1877 (Trichoptera: Leptoceridae): When the taxonomy and phylogeny meet. Zoologischer Anzeiger 293: 233–246. https://doi.org/10.1016/j.jcz.2021.06.005

Quinteiro FB, Calor AR (2012) A new species of *Oecetis* McLachlan, 1877 (Trichoptera: Leptoceridae) from Southeast Brazil: validation of an unpublished species. Zootaxa 3442: 53–57. https://doi.org/10.11646/zootaxa.3442.1.2

Quinteiro FB, Calor AR (2015) A review of the genus *Oecetis* (Trichoptera: Leptoceridae) in the Northeastern Region of Brazil with the description of 5 new species. Plos One, 10(6): e0127357. https://doi.org/10.1371/journal.pone.0127357

Quinteiro FB, Holzenthal RW (2017) Fourteen new species of *Oecetis* McLachlan, 1877 (Trichoptera: Leptoceridae) from the Neotropical region. PeerJ 5: e3753. https://doi.org/10.7717/peerj.3753

QGIS (2023) A Free and Open Source Geographic Information System. Firenze version 3.28. https://qgis.org

Rambaut A (2016) FigTree: Tree Figure Drawing Tool, version 1.4.3. Available at: http://tree.bio.ed.ac.uk (accessed Sept. 2023).

Rambaut A, Drummond AJ, Xie D, Baele G, Suchard MA (2018) Posterior summarisation in Bayesian phylogenetics using Tracer 1.7. Systematic Biology 67: 901–904. https://doi.org/10.1093/sysbio/syy032

Ronquist F, Teslenko M, Mark van der P, Ayres DL, Darling A, Höhna S, Larget B, Liu L, Suchard MA, Huelsenbeck JP (2012) MrBayes 3.2: efficient Bayesian phylogenetic inference and model choice across a large model space. Systematic Biology 61: 539–542. https://doi.org/10.1093/sysbio/sys029

Rosa BB, Melo GAR, Barbeitos MS (2019) Homoplasy-based partitioning out-performs alternatives in Bayesian analysis of discrete morphological data. Systematic Biology 68: 657–671. https://doi.org/10.1093/sysbio/syz001

Schmid F (1998) The insects and arachnids of Canada Part 7. Genera of the Trichoptera of Canada and adjoining or adjacent United States. NRC Research Press, Ottawa, 289 pp.

Sereno PC (2007) Logical basis for morphological characters in phylogenetics. Cladistics 23: 565–587. https://doi.org/10.1111/j.1096-0031.2007.00161.x

Silfvenius AJ (1905) Beiträge zur Metamorphose der Trichopteren. Acta Societatis pro Fauna et Flora Fennica 27: 1–168.

Statzner B (1974) Funktionsmorphologische Studien am Genitalapparat von drei neuen Cheumatopsyche-Arten (Trichoptera, Hydropsychidae). Zoologischer Anzeiger 193: 382–398.

Thomas JA, Frandsen PB, Prendini E, Zhou X, Holzenthal RW (2020) A multigene phylogeny and timeline for Trichoptera (Insecta). Systematic Entomology 45: 670–686. https://doi.org/10.1111/syen.12422

Tobias W (1972) Zur Kenntnis europäischer Hydropsychidae (Insecta: Trichoptera), I. Senckenbergiana biologica 53: 59–89.

Vaidya G, Lohman DJ, Meier R (2011) SequenceMatrix: concatenation software for the fast assembly of multi-gene datasets with character set and codon information. Cladistics 27: 171–180. https://doi.org/10.1111/j.1096-0031.2010.00329.x

Wallace ID, Wallace B, Philipson GN (2003) A key to the case-bearing caddis larvae of Britain and Ireland. Freshwater Biological Association Scientific Publication 61: 1–259.

Walker F (1852) Catalogue of the Specimens of Neuropterous Insects in the Collection of the British Museum, Part I: Phryganides-Perlides. British Museum London, London. https://doi.org/10.5962/bhl.title.9318

Wasserstein RL, Schirm AL, Lazar NA (2019) Moving to a world beyond "p< 0.05". The American Statistician 73: 1–19. https://doi.org/10.1080/00031305.2019.1583913

Wells A (2000) New Australian species of *Oecetis* allied to *O. complexa* Kimmins (Trichoptera: Leptoceridae). Memoirs of Museum Victoria 58(1): 77–88. http://doi.org/10.24199/j.mmv.2000.58.4

Wells A (2004) The long-horned caddisfly genus *Oecetis* (Trichoptera: Leptoceridae) in Australia: two new species groups and 17 new species. Memoirs of Museum Victoria 61: 85–110. http://doi.org/10.24199/j.mmv.2004.61.7

Wells A (2006) A review of Australian long-horned caddisflies in the *Oecetis pechana*-group (Trichoptera: Leptoceridae), with descriptions of thirteen new species. Memoirs of Museum Victoria 63: 107–128. http://doi.org/10.24199/j.mmv.2006.63.13

Wiggins GB (2007) Caddisflies: architects under water. American Entomology 53: 78–85.

Zander RH (2004) Minimal values for reliability of bootstrap and jackknife proportions, decay index, and Bayesian posterior probability. Phyloinformatics 2: 1–13.

Supplementary Material 1

Files S1, S2

Authors: Bonfá-Neto P, Salles FF, Vilarino A (2024)
Data type: .zip
Explanation notes: File S1. Material type and material analyzed standardized in Darwin Core (DWC). — **File S2.** Additional information from distributional records shown on the map (Fig. 5).

Link: https://doi.org/asp.82.e114286.suppl1

Supplementary Material 2

File S3

Authors: Bonfá-Neto P, Salles FF, Vilarino A (2024)
Data type: .pdf
Explanation notes: Material Morphological tree. Single most parsimonious tree generated at TNT with the adjusted K = 15. Branch support values are displayed near the branches: above Relative Bremer support (from branch-swapping of suboptimal trees up to 10 steps longer and relative fit of 0.9%), below in bold Symmetric Resample (100 replicates, with a change probability of 0.33).

Link: https://doi.org/asp.82.e114286.suppl2